

## REVEALING THE JET STRUCTURE OF GRB 030329 WITH HIGH-RESOLUTION MULTICOLOR PHOTOMETRY

J. GOROSABEL,<sup>1</sup> A. J. CASTRO-TIRADO,<sup>1</sup> E. RAMIREZ-RUIZ,<sup>2,3</sup> J. GRANOT,<sup>4</sup> N. CAON,<sup>5</sup> L. M. CAIRÓS,<sup>5</sup>  
E. RUBIO-HERRERA,<sup>6</sup> S. GUZİY,<sup>1</sup> A. DE UGARTE POSTIGO,<sup>1</sup> AND M. JELÍNEK<sup>1</sup>

Received 2005 November 16; accepted 2006 March 3; published 2006 March 20

### ABSTRACT

We present multicolor optical observations of the nearby ( $z = 0.1685$ ) gamma-ray burst GRB 030329 obtained with the same instrumentation over a time period of 6 hours, for a total of an unprecedented 475 quasi-simultaneous *BVR* observations. The achromatic steepening in the optical, which occurs at  $t \sim 0.7$  days, provides evidence for a dynamic transition of the source and can be most readily explained by models in which the GRB ejecta are collimated into a jet. Since the current state-of-the-art modeling of GRB jets is still fraught with uncertainties, we use these data to critically assess some classes of models that have been proposed in the literature. The data, especially the smooth decline rate seen in the optical afterglow, are consistent with a model in which GRB 030329 was a homogeneous, sharp-edged jet, viewed near its edge interacting with a uniform external medium or viewed near its symmetry axis with a stratified wind-like external environment. The lack of short-timescale fluctuations in the optical afterglow flux down to the 0.5% level puts stringent constraints on possible small-scale angular inhomogeneities within the jet or fluctuations in the external density.

*Subject headings:* gamma rays: bursts — ISM: jets and outflows — shock waves

*Online material:* color figure, machine-readable table

### 1. INTRODUCTION

A watershed event occurred on 2003 March 29 when *HETE-2* rapidly localized a long gamma-ray burst (GRB) (Vanderspek et al. 2003). The prompt discovery of the fading optical counterpart (Torii et al. 2003; Price et al. 2003; Uemura et al. 2004; Sato et al. 2003), combined with its exceptional brightness, allowed densely sampled observations of this afterglow (Lipkin et al. 2004 and references therein). At  $z = 0.1685$  (Greiner et al. 2003a), GRB 030329 is the third-closest GRB to date for which an optical afterglow (OA) has been discovered. It is by detailed study of such nearby events that we have learned the most about the range of physical processes relevant to GRBs. GRB 030329 was the first burst to have a secure spectroscopic association with a Type Ic supernova (Stanek et al. 2003; Hjorth et al. 2003; Sokolov et al. 2003), and the monitoring of its afterglow polarization is the best to date (Greiner et al. 2003b). In its early evolution, the GRB 030329 afterglow also provided strong evidence for slow shells with modest Lorentz factors carrying most of the kinetic energy in the relativistic ejecta (Granot et al. 2003).

Follow-up observations within 1.5 hr (Peterson & Price 2003) discovered an OA with  $R \sim 12$  mag, brighter than any OA previously detected at a similar epoch. Soon after, intensive spectroscopic monitoring revealed a supernova, SN 2003dh, with a spectrum very similar to that of SN 1998bw. These observations showed that  $\sim 0.4 M_{\odot}$  of  $^{56}\text{Ni}$ , the parent nucleus of  $^{56}\text{Co}$ , was formed in the explosion, suggesting a progenitor main-sequence mass of 25–40  $M_{\odot}$  (Mazzali et al. 2003). The GRB 030329 afterglow was monitored in the radio, optical,

and X-ray bands. The radio image was resolved by the Very Long Baseline Array (Taylor et al. 2004) and its diameter was measured to be  $\sim 0.2$  pc after 25 days ( $\sim 0.5$  pc after 83 days), indicating an average apparent expansion velocity of  $\sim 5.7c$  ( $\sim 4.1c$ ). This decelerating apparent superluminal expansion agrees with expectations of the standard afterglow theory (Oren et al. 2004). The image size did not change much between 83 and 217 days (Taylor et al. 2005), favoring a uniform external medium and a jet with little lateral spreading. The GRB 030329 light curve indeed showed a panchromatic steepening at about half a day, which has been attributed to a jetlike outflow (Price et al. 2003).

GRB 030329 belongs to a growing group of GRBs for which densely monitored OA light curves show significant deviations relative to a smooth power-law decay—most notably GRB 021004 (Bersier et al. 2003; de Ugarte Postigo et al. 2005) and GRB 011211 (Jakobsson et al. 2004). These deviations are interesting to constrain the activity and identity of the central engine driving the GRB, but they complicate the simple jet interpretation mentioned above. In this Letter, we report observations of the GRB 030329 OA that overcome the previous sampling limitations with a total of an unprecedented 475 high-resolution, quasi-simultaneous *BVR*-band observations obtained with the same instrumentation over a period of 6 hours. Here, for the first time, we establish a detailed multicolor optical light curve around the break time and argue that in concert the data provide good support for the jet interpretation of the light-curve break. The Letter is structured as follows: § 2 details the observations and data analysis, § 3 discusses the physical implications, and our conclusions are summarized in § 4.

### 2. OBSERVATIONS

We commenced observations of the GRB 030329 OA 9.44 hr after the GRB, using the ALFOSC camera at the 2.5 m Nordic Optical Telescope. We continued monitoring with the same instrumentation over a period of 6 hr. The data were taken in sequential cycles of *BVR*-band images. The monitoring is composed of 157 images in *B*, 158 in *V*, and 160 in *R*. In order

<sup>1</sup> Instituto de Astrofísica de Andalucía, CSIC, Apdo. 3004, E-18008 Granada, Spain.

<sup>2</sup> Institute for Advanced Study, Einstein Drive, Princeton, NJ 08540.

<sup>3</sup> *Chandra* Fellow.

<sup>4</sup> Kavli Institute for Particle Astrophysics and Cosmology, Stanford University, 2575 Sand Hill Road, Mail Stop 29, Menlo Park, CA 94025.

<sup>5</sup> Instituto de Astrofísica de Canarias, Calle Vía Láctea, E-38205 La Laguna, Tenerife, Spain.

<sup>6</sup> Sterrenkundig Instituut Anton Pannekoek, Kruislaan 403, NL-1098 SJ Amsterdam, Netherlands.

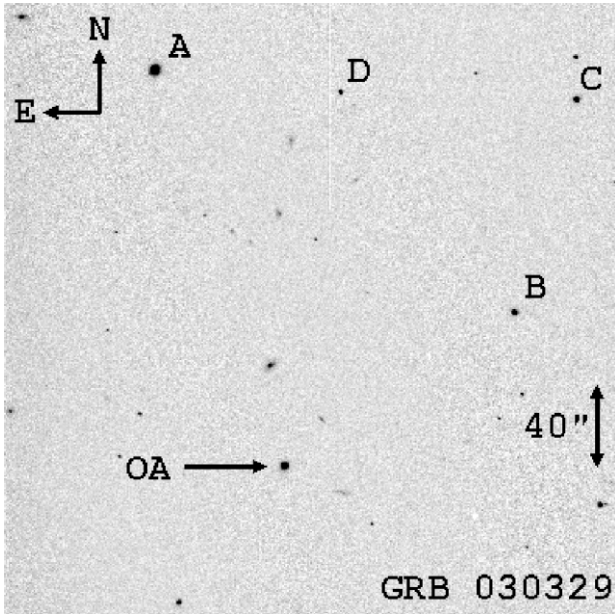


FIG. 1.—*B*-band image of the field centered on the optical afterglow of GRB 030329. The reference stars A, B, C, and D and the OA are indicated.

to enhance the time resolution, the  $2048 \times 2048$  pixel chip of ALFOSC was binned  $2 \times 2$  and trimmed to an  $800 \times 800$  pixel window. The typical exposure time per frame was 20 s, achieving a time resolution (including readout time) of about  $\sim 150$  s between two consecutive images taken in the same band. The photometry is based on aperture photometry routines running under IRAF.

The center of the field of view was selected to include the OA and four reference stars (A, B, C and D; see Fig. 1). The OA magnitude ( $R \sim 15$ ) is similar to those of the reference stars (Henden 2003), showing photometric errors (typically less than 1%) comparable to the OA. Although the air mass during our observations did not reach extreme values ( $\sec z < 1.6$ ), we introduced air-mass–dependent color term corrections to derive the OA *BVR*-band magnitudes. This correction is more prominent at *B* band, reaching an OA flux increment up to 0.007 mag at  $\sec z = 1.6$ . For calibration, at a given aperture four different OA light curves were obtained per filter, each one based on a different reference star. We averaged the residuals of the four light curves, instead of averaging over the individual, calibrated light curves, so that the error of the residuals was not affected by the zero-point uncertainty of the reference stars. This allowed us to decrease the potential dispersion contribution due to the reference stars’ statistical fluctuations. This method provided, for a given photometric aperture, the mean *BVR*-band fluctuations. As a sanity check, the process was repeated for six apertures, ranging from 1 to 2.5 times the stars’ FWHM. The final light curve and the shape of the associated

TABLE 1  
LIGHT-CURVE DATA FOR GRB 030329

MJD	Band	Magnitude
2728.3776157–2728.3777315 .....	<i>B</i>	$15.166 \pm 0.014$
2728.3787153–2728.3788310 .....	<i>R</i>	$14.502 \pm 0.023$
2728.3803472–2728.3805208 .....	<i>B</i>	$15.170 \pm 0.013$
2728.3807870–2728.3809028 .....	<i>V</i>	$14.828 \pm 0.009$

NOTE.—Table 1 is published in its entirety in the electronic edition of the *Astrophysical Journal*. A portion is shown here for guidance regarding its form and content.

residuals (see Fig. 2, *bottom*) were independent of the adopted aperture. The final magnitudes were obtained by averaging the light curves yielded for the six apertures (see Table 1).

The *B*-, *V*-, and *R*-band light curves, along with numerous points from other groups reported in the literature, are plotted in Figure 2, where it is evident that the light curve steepens contemporaneously in all bands between  $\sim 0.3$  and  $\sim 0.9$  days. In order to characterize the shape of the afterglow light curve near the jet break time,  $t_j$ , we fitted the data with the phenomenological Beuermann et al. (1999) function,

$$F(t, \nu) = F_0 \nu^\beta [(t/t_j)^{-\alpha_1 s} + (t/t_j)^{-\alpha_2 s}]^{-1/s} + F_{\text{host}}(\nu), \quad (1)$$

which provides a good description of the data, featuring a smooth transition (whose sharpness is parameterized by  $s$ ) between the asymptotic power-law indices  $\alpha_1$  and  $\alpha_2$  at early and late times, respectively.  $F_{\text{host}}(\nu)$  corresponds to the *BVR*-band host galaxy flux, which was fixed using the magnitudes reported in Gorosabel et al. (2005). Fitting the *B*-, *V*-, and *R*-band data simultaneously yields  $t_j = 0.72 \pm 0.2$  days,  $s = 1.6 \pm 0.7$ ,  $\beta = -0.89$

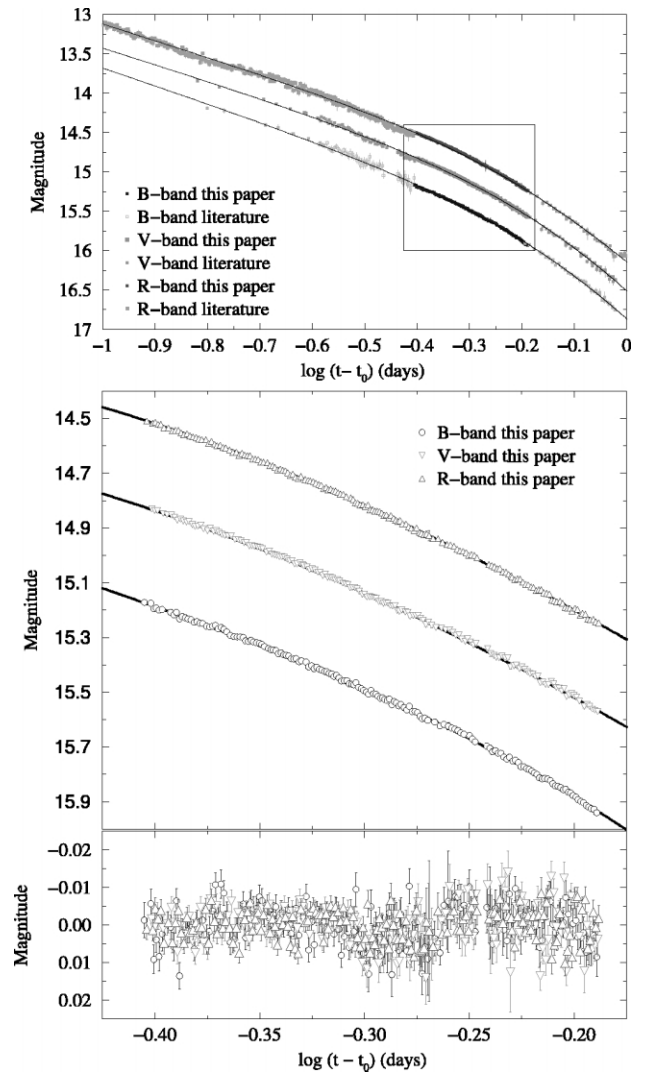


FIG. 2.—*BVR*-band light curves of the GRB 030329 OA. In addition to photometry from our group (*middle*), we have augmented the light curves with data from the literature (*top*). The bottom panel shows the *BVR*-band magnitude residuals with respect to the corresponding Beuermann fits (shown as three solid curves in the middle panel). [See the electronic edition of the *Journal* for a color version of this figure.]

$\pm 0.15$ ,  $\alpha_1 = -0.88 \pm 0.1$ , and  $\alpha_2 = -2.52 \pm 0.3$ , where the uncertainties are formal  $1\sigma$  errors.<sup>7</sup> The  $\chi^2$  for the fit is acceptable: 446 for 638 degrees of freedom. The light curve shows no significant short-timescale variability on top of the smooth trend described by the functional fit above, down to  $\Delta B \sim 0.005$ ,  $\Delta V \sim 0.005$ , and  $\Delta R \sim 0.005$  (i.e.,  $\Delta F/F \lesssim 0.5\%$ ) on timescales  $\geq 150$  s ( $\Delta t/t \geq 10^{-2.5}$ ). The low  $R$ -band dispersion agrees with that found by Urata et al. (2004). A linear fit to  $\beta$  versus  $\log(t - t_0)$  yields a slope of  $-0.037 \pm 0.028$ , consistent with no spectral evolution between 9.44 and 15.56 hr after the burst.

### 3. DISCUSSION

#### 3.1. Evidence for a Jet in GRB 030329

A panchromatic steepening in the OA flux decay, like that reported here in three optical bands ( $BVR$ ) for GRB 030329, was predicted for an outflow collimated into a narrow jet (Rhoads 1999). Such a “jet break” occurs when the Lorentz factor,  $\Gamma$ , of the shocked external medium drops below  $\theta_0^{-1}$ , where  $\theta_0$  is the initial half-opening angle of the jet (Sari et al. 1999). At this stage the edge of the jet becomes visible. In principle, lateral expansion of the jet might also become important when  $\Gamma\theta_0 \sim 1$ , as the edge of the jet and its center come into causal contact. However, hydrodynamic simulations (Granot et al. 2001) show a modest degree of lateral spreading as long as the jet is relativistic, suggesting that the jet break in the light curve is caused primarily because the edge of the jet becomes visible.

At early times,  $t \ll t_j$ , the light curve is given by the spherical solution, where in the optical (depending on the density profile assumed for the external matter)  $\alpha_1 = 3(1-p)/4$  for a uniform density profile and  $\alpha_1 = (1-3p)/4$  for a wind. The closure relation  $\alpha_1 - 3\beta/2 = 0$  is expected for a uniform density ( $=\frac{1}{2}$  for a wind). Our observed value,  $\alpha_1 - 3\beta/2 = -0.45 \pm 0.3$ , favors a uniform density, for which  $p = 1 + 4\alpha_1/3 = 2.2 \pm 0.2p = 1 + 2\beta = 2.78 \pm 0.3$  are marginally consistent. For relativistic lateral spreading of the jet in its own rest frame,  $\alpha_2 = -p$  (Sari et al. 1999). For little or no lateral spreading,  $\alpha_1 - \alpha_2 = -2(d \log \Gamma/d \log t) = (3-k)/(4-k)$  for a power-law external density,  $\rho_{\text{ext}} \propto r^{-k}$ , so that  $\alpha_2 = -3p/4$  for  $k = 0$ . However, the value of  $\alpha$  immediately after the break is smaller than its asymptotic value,<sup>8</sup> underestimating  $\alpha_2$ . Therefore, our measured value of  $\alpha_2 = -2.52 \pm 0.3$  is consistent with this picture. For  $t_j = 0.72 \pm 0.2$  days, we find  $\theta_0 = 0.097(E_{51}/n_0)^{-1/6}$  for  $k = 0$  and  $\theta_0 = 0.13(E_{51}/A_*)^{-1/2}$  for  $k = 2$ . Using the constraints on  $E_{51}/n_0$  ( $E_{51}/A_*$ ) from the radio image size (Granot et al. 2005), we derive<sup>9</sup>  $\theta_0 \sim 0.083\text{--}0.14$  ( $\sim 0.27\text{--}0.55$ ).

The densely monitored observations presented here provide a unique opportunity to critically assess different jet models that have been proposed and to constrain the jet structure and the external density profile. We start with a uniform external medium and consider two models, of increasing complexity. First, we consider a simple semianalytical model (model 1 of Granot & Kumar 2003; see also Ramirez-Ruiz et al. 2005), which neglects lateral spreading. This approximation is consistent with the results of hydrodynamic simulations (Cannizzo et al. 2004), which are also considered here. The advantage of the hydrodynamic

model is a reliable and rigorous treatment of the jet dynamics, which provides insight into the behavior of the jet and light curves. We use equation (1) to determine the sharpness parameter,  $s$ , of the jet break. While the prompt GRB seen by all observers within the initial jet aperture,  $\theta_{\text{obs}} < \theta_0$ , is the same for a uniform jet, the jet break is sharper at smaller  $\theta_{\text{obs}}$  (Granot et al. 2001). For a uniform jet, we find  $s$ -values of 7.3, 4.4, 1.9, 1.1, and 1.6 for  $\theta_{\text{obs}} = (0, \frac{1}{4}, \frac{1}{2}, \frac{3}{4}, 1)\theta_0$ , respectively. While the basic light-curve features for  $\theta_{\text{obs}} < \theta_0$  are similar in both models, the hydrodynamic model gives sharper breaks; for example, we find  $s$ -values ranging from  $^{10} s(\theta_{\text{obs}} = 0) \sim 10$  to  $s(\theta_{\text{obs}} = \theta_0) \sim 1$ .

For a wind external density profile ( $k = 2$ ), the jet break is smoother, both because the Lorentz factor decreases more slowly with time (Kumar & Panaitescu 2000) and because the limb brightening of the afterglow image is weaker (Granot & Loeb 2001) as compared with a uniform external medium ( $k = 0$ ). For the uniform-jet model, we find  $s = (2.2, 1.8, 1.2, 0.8, 1.1)$  for  $\theta_{\text{obs}} = (0, \frac{1}{4}, \frac{1}{2}, \frac{3}{4}, 1)\theta_0$ . While the slow change in image size observed between 83 and 217 days favors a uniform external medium (Taylor et al. 2005), the sharpness change does not. The relatively smooth break in GRB 030329, with  $s = 1.6 \pm 0.7$ , suggests  $\theta_{\text{obs}}/\theta_0 \sim 0.7\text{--}1$  ( $\leq 0.7$ ) for  $k = 0$  ( $k = 2$ ). However, a large fraction of OAs show evidence for sharper breaks (Zeh et al. 2006), with  $s$ -values consistent with lower values of  $\theta_{\text{obs}}/\theta_0$  for  $k = 0$ , but are too sharp for any viewing angle for  $k = 2$ .

#### 3.2. GRB 030329 and Its Variability

GRB 030329 belongs to a growing group of bursts for which densely monitored light curves show significant “bumps” and “wiggles” relative to a simple power-law decay. Figure 3 shows the temporal evolution of the variability timescale,  $\Delta t/t$ , of the various wiggles observed in the GRB 030329 light curve, together with other reported variations from a simple power-law decay in X-ray and GRB OAs. The short-term wavelike behavior of the GRB 030329 optical light curve is unprecedented. The early OA wiggle seen at  $t \sim 10^4$  s (Sato et al. 2003) could be interpreted as a result of the shock wave encountering an external medium of variable density (see, e.g., Wang & Loeb 2000; Ramirez-Ruiz et al. 2001; Lazzati et al. 2002). The pronounced bumps between a day and a week, however, are most readily explained by refreshed shocks, that is, slower shells that were ejected from the source near the end of the GRB and caught up with the afterglow shock at a later time, when the latter decelerated to slightly below the shells’ Lorentz factor (Granot et al. 2003). These shells collide with the shocked fluid behind the afterglow shock and increase its energy (Rees & Mészáros 1998; Panaitescu et al. 1998; Nakar et al. 2003; Heyl & Perna 2003).

Figure 3 shows that while the OA shows substantial variability at  $t \geq 10^5$  s after the burst, we can set a very strict upper limit on the variability shortly before the onset of the wavelike behavior of the optical light curve,  $\Delta F/F \lesssim 5 \times 10^{-3}$  on timescales  $10^{-2.5} \leq \Delta t/t \leq 0.25$ . The low level of variability before 1 day constrains both the possible angular inhomogeneity within the afterglow shock and density variations in the external medium. Let us consider variations in the energy per solid angle  $E_{\text{iso}}$  (or external density  $n$ ) on a typical angular (or length) scale  $\theta_E$  ( $l$ ) that cause a fractional change  $\Delta F_0/F_0$  in the local emission from each such small region.<sup>11</sup> The total

<sup>7</sup> Including measurements by other groups (see Fig. 2) before and after our observations results in a slightly sharper break,  $s = 2.3 \pm 0.3$ .

<sup>8</sup> This has been shown in numerical and semianalytic (Rossi et al. 2004) studies and occurs because as the edge of the jet becomes visible, we first start “missing” the outer part of the afterglow image, which is limb-brightened (Granot et al. 1999).

<sup>9</sup> We take into account an increase in energy by a factor of  $\sim 10$  due to refreshed shocks that occurred between  $t_j$  and the image size measurements.

<sup>10</sup> The values given here are for  $p = 2.2$ , which is appropriate for GRB 030329. Generally, we expect a sharper jet break (larger  $s$ ) for large values of  $p$  (Rossi et al. 2004).

<sup>11</sup> Since in our case  $F_e \propto n^{1/2} E_{\text{iso}}^{(3+p)/4}$ , a larger fractional change in the density is needed in order to produce the same variation in flux.

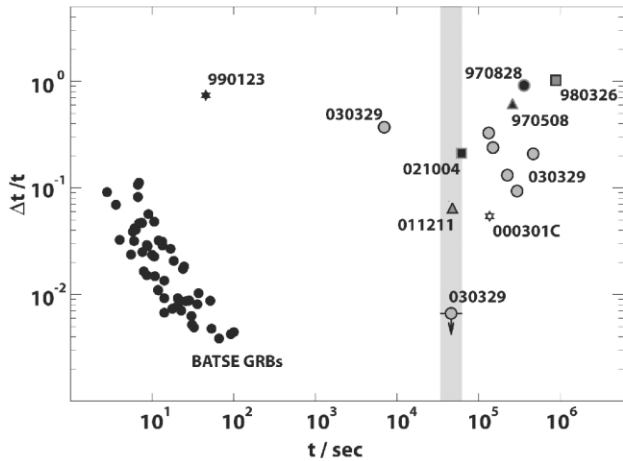


FIG. 3.—Evolution of the variability,  $\Delta t/t$ , of the GRB 030329 OA (gray circle at  $t \lesssim 10^4$  s, Sato et al. [2003]; circle in shaded region, this Letter; gray circles at  $t > 10^5$  s, Lipkin et al. [2004]). Reported variations from a simple power-law decay in the X-ray afterglows of GRB 970508 (Piro et al. 1998) and GRB 970828 (Yoshida et al. 1998) and in the OAs of GRB 980326 (Bloom et al. 1999), GRB 990123 (Akerlof et al. 1999), GRB 011211 (Jakobsson et al. 2004), GRB 021004 (Bersier et al. 2003), and GRB 000301C (Garnavich et al. 2000) are also illustrated. The filled symbols are long, complex BATSE GRBs for which  $\Delta t$  has been estimated from the width of the autocorrelation function (Fenimore et al. 1999), and  $t$  is the GRB duration. This figure demonstrates that while the GRB 030329 OA displays substantial variability at  $t \gtrsim 10^5$  s after the burst, we observe (shaded region) no significant variability,  $\Delta t/t \lesssim 10^{-2.5}$ , shortly before the onset of the wavelike behavior.

number of regions contributing to the total observed flux is  $N \sim (\Gamma\theta_E)^{-2} [N \sim \Gamma^{-2}(R/l)^3]$ , and since around the jet break time  $\Gamma \sim \theta_0^{-1}$ , we have  $N \sim (\theta_0/\theta_E)^2 [N \sim \theta_0^2(R/l)^3]$ . We expect the fluctuations in the total observed flux on a time-scale  $\Delta t$  to be of order  $\Delta F/F \sim N^{-1/2}(\Delta t/t)^{1/2}(\Delta F_0/F_0)$ . For

our limits, this implies  $N^{1/2} \gtrsim 100(\Delta F_0/F_0)$ , that is,  $l/R \lesssim 10^{-2}(\theta_0/0.1)^{2/3}(\Delta F_0/F_0)^{-2/3}$ , where  $R(t_j) \approx 5.4 \times 10^{17}(E_{50}/n_0)$  cm, or  $\theta_E \lesssim 10^{-3}(\theta_0/0.1)(\Delta F_0/F_0)^{-1}$ .

#### 4. CONCLUSIONS

We report on high-resolution photometric observations of the GRB 030329 OA obtained with the same instrumentation over a time period of 6 hours for a total of 475 quasi-simultaneous *BVR*-band measurements with typical statistical photometric errors below 0.005 mag. Our data, to our knowledge, constitute the most complete and dense sampling of the jetlike behavior of a GRB afterglow to date. Our well-sampled multicolor light curve is well described by a physical model in which the ejecta are collimated in a jet. We conclude that the observations, especially the smooth decline rate seen in the OA, are consistent with a model in which GRB 030329 was a sharp-edged GRB jet. We consider both a uniform and a wind density profile. While both the observed evolution of the image size and the relation between the observed spectral and temporal indices favor a uniform medium, both models are consistent with smooth jet break in our data. Moreover, we derive strict upper limits on the afterglow short-timescale variability during our observations, of  $\lesssim 0.5\%$ , which put strong limits on possible fluctuations in the energy per solid angle within the jet and in the external density. Evolving photometric properties provide a unique diagnostic tool for GRB studies, and the complex light curve of the GRB 030329 OA emphasizes that data should be acquired with high sampling frequency.

This work is supported by the Institute for Advanced Study and NASA through a *Chandra* Fellowship, award PF3-40028 (E. R.-R.), under contract DE-AC03-76SF00515 (J. G.), and by the Spanish Ministry of Science through programs ESP 2002-04124-C03-01 and AYA 2004-01515.

#### REFERENCES

- Akerlof, C., et al. 1999, *Nature*, 398, 400  
 Bersier, D., et al. 2003, *ApJ*, 584, L43  
 Beuermann, K., et al. 1999, *A&A*, 352, L26  
 Bloom, J. S., et al. 1999, *Nature*, 401, 453  
 Cannizzo, J. K., Gehrels, N., & Vishniac, E. T. 2004, *ApJ*, 601, 380  
 de Ugarte Postigo, A., et al. 2005, *A&A*, 443, 841  
 Fenimore, E. E., Cooper, C., Ramirez-Ruiz, E., Sumner, M. C., Yoshida, A., & Namiki, M. 1999, *ApJ*, 512, 683  
 Garnavich, P. M., Loeb, A., & Stanek, K. Z. 2000, *ApJ*, 544, L11  
 Gorosabel, J., et al. 2005, *A&A*, 444, 711  
 Granot, J., & Kumar, P. 2003, *ApJ*, 591, 1086  
 Granot, J., & Loeb, A. 2001, *ApJ*, 551, L63  
 Granot, J., Miller, M., Piran, T., Suen, W.-M., & Hughes, P. A. 2001, in *Gamma-Ray Bursts in the Afterglow Era*, ed. E. Costa, F. Frontera, & J. Hjorth (Berlin: Springer), 312  
 Granot, J., Nakar, E., & Piran, T. 2003, *Nature*, 426, 138  
 Granot, J., Piran, T., & Sari, R. 1999, *ApJ*, 513, 679  
 Granot, J., Ramirez-Ruiz, E., & Loeb, A. 2005, *ApJ*, 618, 413  
 Greiner, et al. 2003a, *GCN Circ.* 2020  
 ———. 2003b, *Nature*, 426, 157  
 Henden, A. 2003, *GCN Circ.* 2082  
 Heyl, J. S., & Perna, R. 2003, *ApJ*, 586, L13  
 Hjorth, J., et al. 2003, *Nature*, 423, 847  
 Jakobsson, P., et al. 2004, *NewA*, 9, 435  
 Kumar, P., & Panaitescu, A. 2000, *ApJ*, 541, L9  
 Lazzati, D., Rossi, E., Covino, S., Ghisellini, G., & Malesani, D. 2002, *A&A*, 396, L5  
 Lipkin, Y. M., et al. 2004, *ApJ*, 606, 381  
 Mazzali, P. A., et al. 2003, *ApJ*, 599, L95  
 Nakar, E., Piran, T., & Granot, J. 2003, *NewA*, 8, 495  
 Oren, Y., Nakar, E., & Piran, T. 2004, *MNRAS*, 353, L35  
 Panaitescu, A., Mészáros, P., & Rees, M. J. 1998, *ApJ*, 503, 314  
 Peterson, B. A., & Price, P. A. 2003, *GCN Circ.* 1985  
 Piro, L., et al. 1998, *A&A*, 331, L41  
 Price, P. A., et al. 2003, *Nature*, 423, 844  
 Ramirez-Ruiz, E., Dray, L. M., Madau, P., & Tout, C. A. 2001, *MNRAS*, 327, 829  
 Ramirez-Ruiz, E., Granot, J., Kouveliotou, C., Woosley, S. E., Patel, S. K., & Mazzali, P. A. 2005, *ApJ*, 625, L91  
 Rees, M. J., & Mészáros, P. 1998, *ApJ*, 496, L1  
 Rhoads, J. E. 1999, *ApJ*, 525, 737  
 Rossi, E. M., Lazzati, D., Salmonson, J. D., & Ghisellini, G. 2004, *MNRAS*, 354, 86  
 Sari, R., Piran, T., & Halpern, J. P. 1999, *ApJ*, 519, L17  
 Sato, R., Kawai, N., Suzuki, M., Yatsu, Y., Kataoka, J., Takagi, R., Yanagisawa, K., & Yamaoka, H. 2003, *ApJ*, 599, L9  
 Sokolov, V. V., et al. 2003, *Bull. Spec. Astrophys. Obs.*, 56, 5  
 Stanek, K. Z., et al. 2003, *ApJ*, 591, L17  
 Taylor, G. B., Frail, D. A., Berger, E., & Kulkarni, S. R. 2004, *ApJ*, 609, L1  
 Taylor, G. B., Momjian, E., Pihlström, Y., Ghosh, T., & Salter, C. 2005, *ApJ*, 622, 986  
 Torii, K., et al. 2003, *ApJ*, 597, L101  
 Uemura, M., et al. 2004, *PASJ*, 56, S77  
 Urata, Y., et al. 2004, *ApJ*, 601, L17  
 Vanderspek, R., et al. 2003, *GCN Circ.* 1997  
 Wang, X., & Loeb, A. 2000, *ApJ*, 535, 788  
 Yoshida, A., Namiki, M., Otani, C., Kawai, N., Murakami, T., Ueda, Y., Shibata, R., & Uno, S. 1998, in *AIP Conf. Proc.* 428, *Gamma-Ray Bursts*, ed. C. A. Meegan, R. D. Preece, & T. M. Koshut (Woodbury, NY: AIP), 441  
 Zeh, A., Klöse, S., & Kann, D. A. 2006, *ApJ*, 637, 889